

Research Article

# Determination of Mountain Equivalent Rainstorm (MER) in Qinba Mountain Area Based on TRMM

**Khem Chunpanha** , **Yan Baowen\*** 

College of Water Conservancy and Architectural Engineering, Northwest A&F University, Yangling, China

## Abstract

The study of extreme precipitation is a significant aspect for investigating rainstorms, flash floods, and unpredictable disasters. Qinba mountain, Shaanxi province, China, is sensitive to extreme climate and rainstorm events. It is crucial to investigate the feature of precipitation extremes in this region with satellite data. According to this, the paper using the 1Day extreme precipitation datasets of TRMM and rain-gauge to calculate the mountain rainstorm, then the statistical metrics (CC, MBE, RMSE) was used in validation as the performance measure. The 1Day, 3Day, 5Day, and 7Day extreme precipitation was identified by the 95<sup>th</sup> percentile method. Thus to determine the Mountain Equivalent Rainstorm (MER). As the results, (1) Based on the comparison, the TRMM satellite product can capture the extreme precipitation mostly at the station below 433m ( $R^2 > 0.5$ ) for 5Day datasets, while 7Day datasets reveal contrast patterns. (2) By applying the MER concept, the TRMM-based and gauge-based ratio revealed a similar pattern of mountain rainstorms at higher elevations and slightly different in the middle region. The mountain rainstorm amount was double the extreme rainfall at a higher elevation. Therefore, the defined extreme precipitation characteristics can assist the disaster risk reduction and mitigation strategy in the Qinba mountain of Shaanxi Province, China, and also provide a reference for improving the satellite algorithm in extreme precipitation measurement.

## Keywords

Mountain Equivalent Rainfall, Extreme Precipitation, TRMM, Validation, Qinba Mountain Area

## 1. Introduction

Severe precipitation is constantly related to various disasters [1], especially in mountain area, and generated natural disasters in recent years more than ever before with direct or indirect detrimental consequences [2, 3]. Tragic landslides, devastated soil erosion, destruction of infrastructures, ruining of agricultural production, and damaging infrastructure is often the destroyed consequences of the variation of extreme events. One of the extreme events which are the most sensitive to climate change is the trend and pattern of excessive precipitation [4]. And analyzing extreme precipitation events

is beneficial to recognize both the intense hazard region and preparation of water-related disaster management [5, 6]. Particularly, understanding extreme precipitation is an essential factor for projecting the frequency and intensity, and for limiting the damage caused by extreme events. In addition, mountainous extreme precipitation is defined as the most dangerous hazard worldwide [7, 8].

The Qinba mountain, a sensitive place to climate change, is located in China's transitional north and south climate zone and is also the water source of the Middle Route Project of

\*Corresponding author: yanbaowen2000@163.com (Yan Baowen)

**Received:** 16 May 2024; **Accepted:** 6 June 2024; **Published:** 19 June 2024



South to North Water Transfer in China [9]. Qinba mountain area in southern Shaanxi province has many advantages in resources, tourism, and agriculture, which are important areas of economic development in Shaanxi Province [10]. So, being a traditional mountainous agglomeration region and most

influenced by extreme precipitation events, it is necessary to reveal the characteristics of extreme precipitation of this area. The characteristic of extreme precipitation in the Qinba mountain area will improve understanding and prediction of trends of future extreme climate change.

## 2. Data and Method

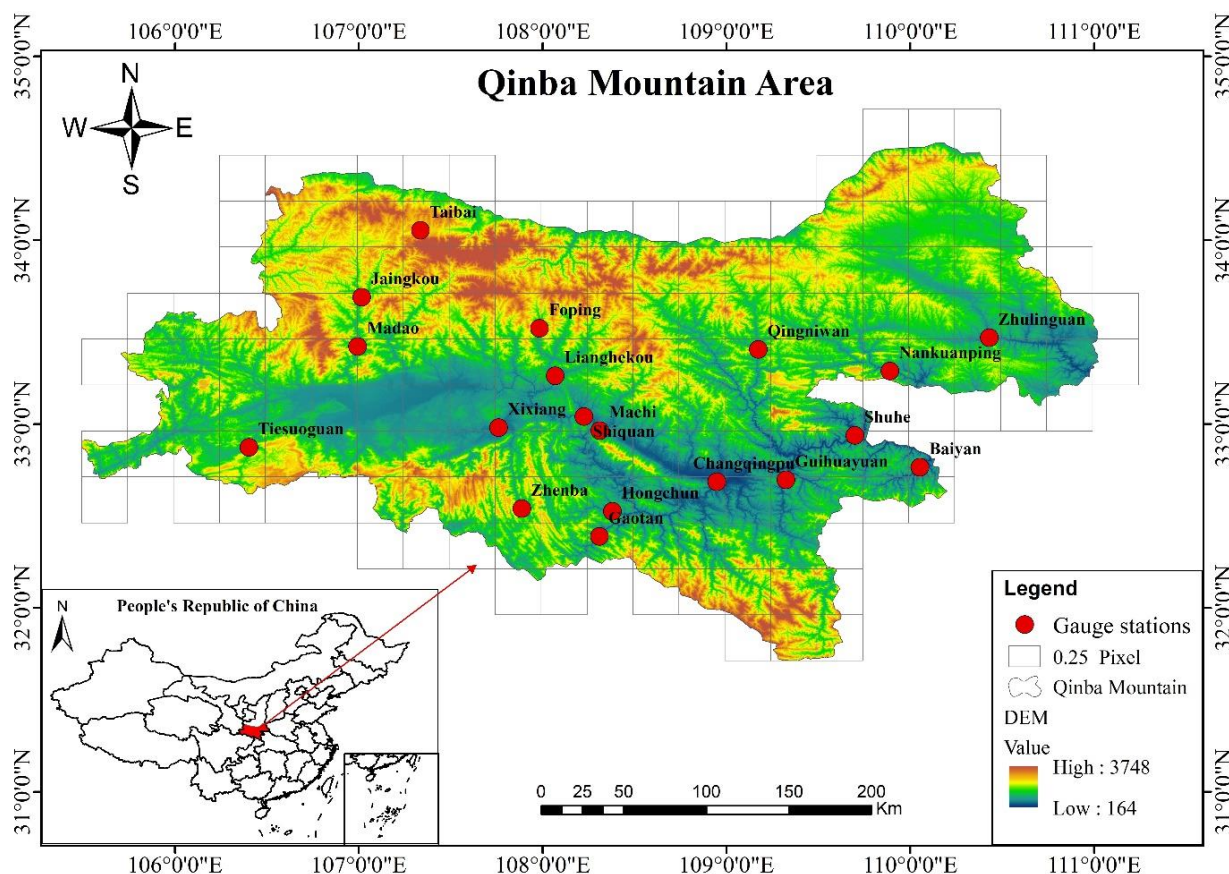


**Figure 1.** The spatial distribution of gauge station and the geographical elevation pattern at the Qinba area.

### 2.1. Study Area

Located at the boundary line between the north and south parts of China, the Qinba Mountain (31°42'–35°N, 105°46'–111°15' E) particularly lies in the Southern part of Shaanxi Province and it is formed at an early Mesozoic progeny by the collision between the Yangtze River in South China and North China [11] (Figure 1). This mountain region dominates approximately 77,000 km<sup>2</sup> of the Shaanxi province. The terrain is undulating, with an altitude of 164 to 3748m, an average of 1175m, and a standard deviation of 486m [12, 13]. And the digital elevation model (DEM) data with 90m spatial resolution was downloaded from: <https://srtm.csi.cgiar.org/>.

### 2.2. Data Collection

#### 2.2.1. Rain Gauge Data

The rain gauge datasets is the observation in which used for ground validation against with corresponding down-scaled precipitation. The whole daily-timescale datasets is originally from the Shaanxi Water Resource Exploration Bureau. There are 19 hydrology stations, which were recorded from January 1<sup>st</sup> 1998 to December 31<sup>st</sup> 2014, and were arranged through Excel and MATLAB software.

#### 2.2.2. TRMM Satellite Precipitation Data

The cooperated project between NASA of the United States and JAXA (the Japan Aerospace Exploration Agency) initi-

ated the satellite precipitation products, namely, TRMM (Tropical Rainfall Measuring Mission) in late 1997 and ceased the operation in April 2015, then reactivated into the earth orbit later that year to observe the global precipitation. The TRMM version 7 was attached with precipitation- detection equipment during the quasi-global monitoring mission, including VIRS (the Visible Infrared Radiometer), TMI (TRMM Microwave Image), CERES (Cloud and Earth Radiant Energy Sensor), LIS (Lightning Imaging Sensor), and PR (the first space borne precipitation radar). Among several precipitation retrieval algorithms, TMPA (Tropical Rainfall Measuring Mission Multi-Satellite Precipitation Analysis products) has been developed through a synthesis of observation from rainfall gauge analyses and satellite-based microwave and infrared sensors. The TMPA algorithm performed the precipitation monitoring on the earth coverage of 50°N-S with a spatial resolution of 0.25° x 0.25° (16 Km) precipitation estimate [14]. In this study, the first decommission period of TRMM is selected for the study with the TRMM products, named, TRMM-3B42. The satellite-based precipitation datasets was obtained from the data archive of the GES DISC website: <https://disc.gsfc.nasa.gov/>.

Since the operation of TRMM has been finished, the related inquiry may propose why this research is conducting that the TRMM-3B42 datasets is no further continued. There are several explanations related to this: (1) there are few verification in confirming the down-scaling method for satellite-based precipitation products with local-spatial variation explanatory variables, and (2) the consequence of the research could be the hypothesis for strengthening the utilizing satellite products in hydrology, meteorology and water resources management, and (3) this study could be valuable guidance for other research in evaluating or applying satellite precipitation product, especially in term of satellite development. Thus, this research strongly supports improving the satellite resolution for further study in this region and platform down scaling for hydrology issues in other areas.

## 2.3. Research Method

### 2.3.1. Determine Extreme Precipitation

The definition of extreme precipitation is identified by precipitation threshold, in which the daily precipitation amount exceeds the precipitation threshold is identified as extreme precipitation; However, the selection of threshold acquires the probability distribution function for extreme precipitation. The long-term percentile of daily precipitation series from 1998 to 2014 for both gauge station and satellite data were accumulated to form the 1Day, 3Day, 5Day, and 7Day. These datasets are applied based on the Bonsal percentile method to define the threshold for this study. In addition, the distribution of extreme 5Day and 7Day datasets was further analyzed to compare the satellite in capturing extreme precipitation.

The formula of this method is expressed as:

$$P = \frac{(m-0.31)}{(n+0.38)} \quad (1)$$

Where, P is the probability of which random number is less than or equal to the critical value  $Y_m$ ; n is the total number of precipitation data; m is also a critical point divided the data series into two parts where the rank order of  $Y_m$  is located.

In the study, the long-term 95<sup>th</sup> percentile method is selected to define a threshold value for four different extreme precipitation scenarios, as 1Day (daily), 3Day, 5Day, and 7Day precipitation. According to the Bonsal percentile method, the extreme precipitation identification is designed as the following procedure:

- 1) The n precipitation data series are first ranked in ascending order  $Y_1, Y_2, Y_3, \dots, Y_{(m-1)}, Y_m, Y_{(m+1)}, \dots, Y_n$  according to the precipitation value itself.
- 2) Define the critical point ( $Y_m$ ), which separated data into two different parts, depending on percentile value.
- 3) Calculation of linear interpolation between the  $Y_{(m+1)}$  and  $Y_{(m-1)}$  if  $Y_m$  isn't located on the specific rank value. Then, the threshold value is defined.
- 4) The extreme precipitation datasets of 1D, 3D, 5D, and 7D are prepared according to the defined threshold.

### 2.3.2. Mountain Rainstorm Validation

Heavy rain is the main reason for the formation of landslides and debris flow, and the critical value of heavy rain that induces landslide and debris flow is varied according to different locations. In this study, the mountain equivalent rainfall concept is used to observe and verify the presence of mountain equivalent rainstorms according to the result of the extreme precipitation datasets. Both satellite and gauge measurement precipitation were applied with the mountain equivalent rainfall concept to define the number of mountainous natural hazards.

The concept of *Mountain Equivalent Rainfall* described the relationship between rainstorms, which leads to natural disasters, between plain and mountainous regions [15, 16]. Topography is the potential energy basis of landslide and debris flow, especially in the transition area of the first and second steps and the large area of the second steps. To express the contribution of altitude and the probability of occurrence of landslides and mudslides, the Gaussian expression is applied:

$$G(h) = \frac{1}{1 + e^{\frac{1}{2} \left( \frac{h-1300}{400} \right)^2}} \quad (2)$$

Where h: is the altitude of rainfall station (m).

Topography is the static spatial effect of landslide and debris flow, while the time effect is more dynamic. Affected by the monsoon climate, mountain rainfall has continuity, and potential rainfall is closely related to landslides and debris flows [17, 18]. The potential rainfall can express as:

$$R_{PR} = \sum_{d=0}^4 (0.84^d \times R_d) \quad (3)$$

Where  $R_{PR}$ : the potential rainfall of landslides and debris flows caused by continuous rainfall at rainfall station (mm);  $R_d$ : current rainfall at the specific data ( $R_{d=0}$ : rainfall of present-day,  $R_{d=1}$ : rainfall of one day before the present day, and  $R_{d=4}$ : rainfall of four days before present day).

The relationship between rainfall at different altitudes, current rainfall, previous rainfall, and altitude as factors forms a non-linear function expression. This expression is called Mountain Equivalent Rainfall:

$$R_{MER} = R_{CR} + 2R_{PR}G(h) \quad (4)$$

Where  $R_{MER}$ : mountain equivalent rainfall (mm);  $R_{CR}$  (current rainfall): rainfall for 24 hours measures at the rainfall station (mm);  $R_{PR}$ : potential rainfall (mm);  $G(h)$ : the Gaussian expression.

### 3. Extreme Precipitation Induced Disasters Based on Gauge Datasets

Extreme precipitation is one of the consequences of climate change and global warming. Disasters, landslides, and debris flow happen frequently due to the affection of the number of extreme precipitations, mostly in mountain areas. Plus, the geographical condition, altitude, is also a crucial factor leading to landslide and debris flow. Figure 2 demonstrated the average ratio value of gauge-based extreme precipitation to gauge-based mountain rainstorm amount over the long-term timescale from 1998 to 2014 in the Qinba mountain area. According to the figure, it can be indicated that after applying the mountain equivalent rainfall (MER) concept the gauge extreme precipitation value is double the amount of precipitation in higher elevation, and lower elevation has a slight variation of precipitation amount. It can be assumed that the same amount of mountain rainstorm at lower elevations cannot produce debris and landslide in mountain areas; however, it can affect the locals in that area with its extreme characteristics. Based on the figure, the higher ratio value was found in the west part due to the higher elevation of this region, while the east part of Qinba found.

**Table 1.** The value of extreme precipitation and mountain equivalent rainfall based on gauge datasets.

Stations	Elevation (m)	Extreme precipitation (mm)	Mountain Equivalent Rainstorm (mm)	Ratio value
Shuhe	207	44.86	47.59	1.06
Baiyan	234	48.64	52.36	1.08
Changqingpu	253	50.45	57.83	1.09
Guihuayuan	261	45.02	49.1	1.09
Hongchun	349	59.74	69.84	1.17
Gaotan	369	63.42	75.47	1.19
Shiquan	386	53.81	65.22	1.21
Machi	397	50.2	60.67	1.21
Zhulinguan	420	47.08	57.69	1.23
Xixiang	433	48.99	61.33	1.25
Nankuanping	584	48.15	67.74	1.42
Qingniwan	585	43.21	64.8	1.52
Madao	672	46.66	75.68	1.64
Zhenba	699	75.34	135.51	1.83
Tiesuoguan	741	51.89	93.26	1.83
Foping	831	52.74	104.29	2.00
Jiangkou	889	41.47	84.14	2.06
Lianghekou	1336	49.8	123.53	2.53
Taibai	1558	45.39	99.97	2.23

The station with elevations from 831 to 1558m (Foping, Jiangkou, Lianghekou, Taibai) showed the mountain equivalent rainstorm between 104.29 mm, 84.14 mm, 123.53mm, 99.97 mm for station-based datasets, respectively, and the ratio value between 2 to 2.53, which indicated the mountain rainstorm amount was twice the gauge extreme precipitation amount. Meanwhile, the station with elevations of 585 m to 699 m showed the equivalent mountain rainstorm of 64.8mm, 75.68 mm, and 78.5 mm at Qingniwan, Madao, and Zhenba,

respectively, and the ratio ranged between 1.52 to 1.83. The stations at elevations 349 to 584m were defined the mountain equivalent rainstorm with 69.84 mm, 75.47 mm, 65.22 mm, 65.22 mm, 60.67 mm, 57.69 mm, 61.33 mm, 67.74 mm at Hongchun, Gaotan, Shiquan, Machi, Zhulinguan, Xixiang, Nankuanping, and ratios between 1.17 to 1.42, while the ratio value between 1.06 to 1.09 was found at the lowest part of the Qinba area (207 to 253m).

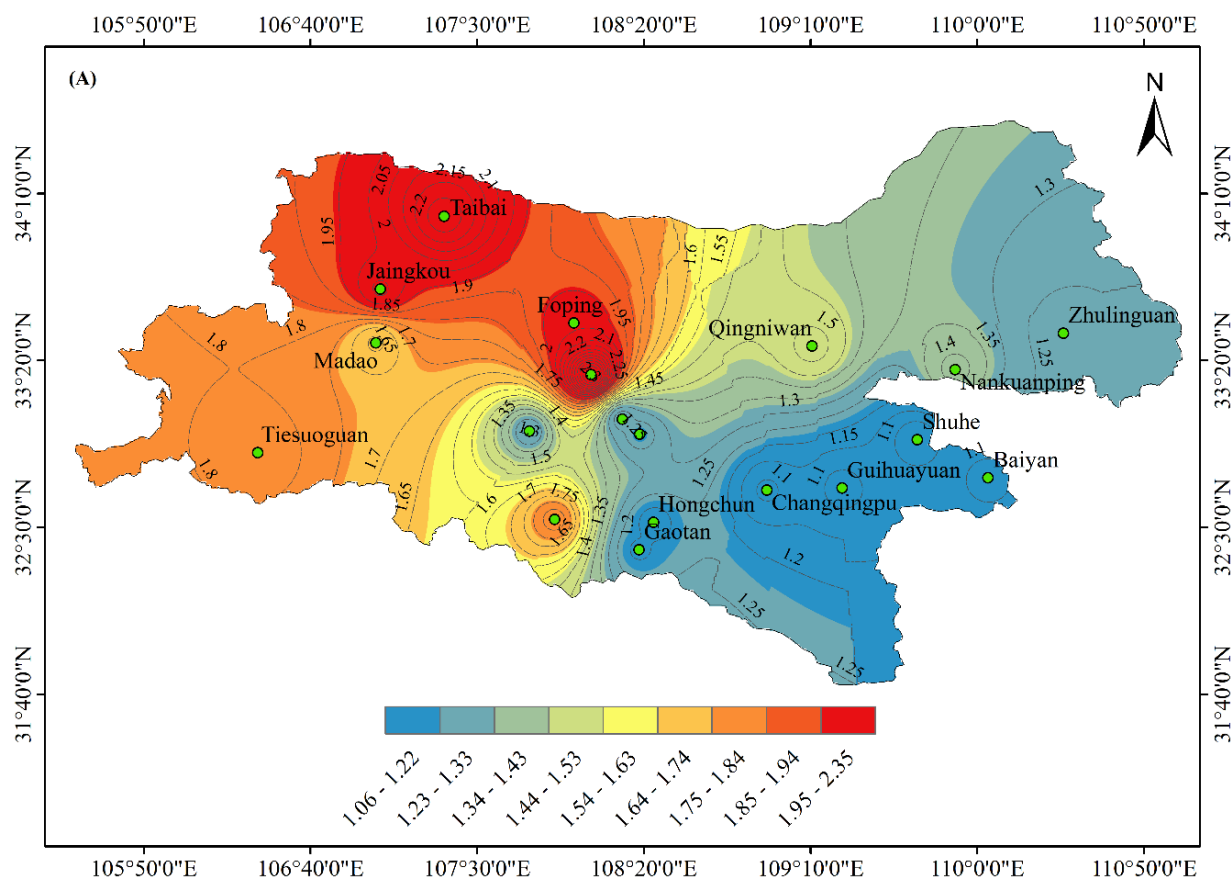


**Figure 2.** The spatial distribution of ratio value between extreme precipitation and mountain rainstorm over the Qinba region.

#### 4. Extreme Precipitation Induced Disasters Based on Satellite Datasets

The satellite algorithm is crucial for measuring precipitation due to its vast variety of temporal and spatial scales globally. In addition, the assessment of satellite capability to capture extreme precipitation is also taken into account for this study. The average ratio value of rainstorm to satellite

extreme precipitation between 1998 to 2014 at Qinba mountain was shown in Figure 3. According to the plot below, the overall ratio value fluctuated between 1.1 to 2.33. The results expressed that the extreme precipitation of the western Qinba region turned into twice the amount of precipitation after the application of the MER concept. The capturing precipitation of the satellite was lower than the ground measurement, so the satellite-based ratio value was also lower. The higher ratio value was found in the west part of the study area, while the east part of Qinba with lower elevation found lower ratio.

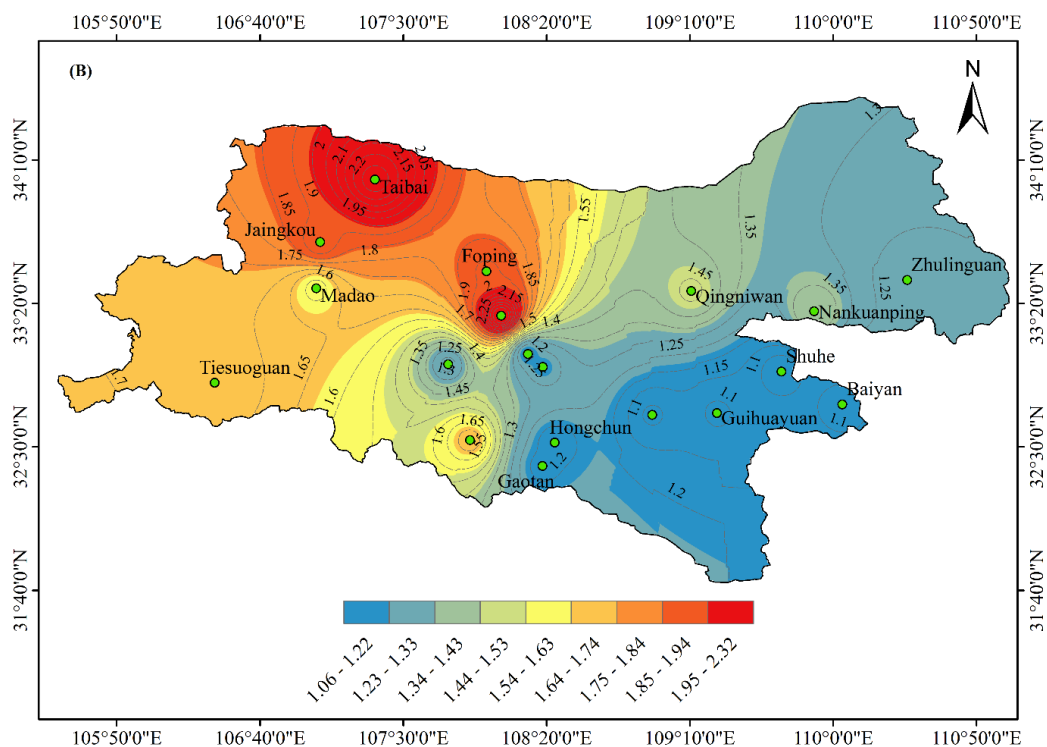


Figure 3. The spatial distribution of ratio value between extreme precipitation and mountain rainstorm over the Qinba region.

Table 2. The value of extreme precipitation and mountain equivalent rainstorm based on satellite data.

Stations	Elevation (m)	Extreme precipitation (mm)	Mountain Equivalent Rainstorm (mm)	Ratio value
Shuhe	207	45.58	48.32	1.06
Baiyan	234	41.74	44.66	1.07
Changqingpu	253	53.96	58.65	1.09
Guihuayuan	261	45.94	49.97	1.09
Hongchun	349	56.63	65.63	1.16
Gaotan	369	58.73	69.19	1.18
Shiquan	386	56.67	67.13	1.18
Machi	397	56.33	67.65	1.20
Zhulinguan	420	39.95	48.7	1.23
Xixiang	433	56.50	69.64	1.23
Nankuanping	584	41.48	57.52	1.40
Qingniwan	585	41.75	60.4	1.46
Madao	672	43.62	68.56	1.58
Zhenba	699	54.96	91.96	1.68
Tiesuoguan	741	49.95	85.67	1.74
Foping	831	44.75	84.65	1.91
Jiangkou	889	43.48	83.81	1.94
Lianghekou	1336	47.69	109.27	2.33
Taibai	1558	36.35	80.42	2.23

Meanwhile, the ratio value was increased according to the increase in elevation. The elevation 207 m to 253 m showed a slight increase of mountain equivalent rainstorm amount with 48.32 mm, 44.66 mm, and 58.65 mm at Shuhe, Baiyan, and Changqingpu, respectively, which ratio value ranges from 1.06 to 1.09; while higher elevations from 349m to 420m indicated the ratio value between 1.16 to 1.23 and the mountain equivalent rainstorm found at Hongchun, Gaotan, Shiquan, Machi, Zhulinguan with 65.63 mm, 69.19 mm, 67.13 mm, 67.65 mm, and 58.78 mm, respectively. The medium elevation between 584 m to 884 m showed a ratio between 1.4 to 1.94 with mountain equivalent rainstorms of 60.4mm, 68.56mm, 91.96mm, 85.67 mm, 84.65 mm, and 83.81 mm, respectively. Lianghekou station was the station with a high ratio value and had a mountain equivalent rainstorm of 109.27 mm.

## 5. Conclusion

The *Mountain Equivalent Rainfall* concept was applied to determine the mountain equivalent rainstorm of both gauge-based and satellite-based datasets. Results received as:

- 1) Both datasets revealed that the mountain equivalent rainstorm is related to the elevation of the stations. The higher elevation indicated the higher mountain equivalent rainstorm amounts.
- 2) MER concept demonstrated that the ratio between extreme precipitation and mountain rainstorm amounts range from 1.1 to 2.05 and 1.1 to 2.04 for gauge-based and satellite-based datasets. The ratio showed a higher value at the higher elevation for both datasets. The difference between those was the satellite ratio value lower than the gauge in the middle area of the study.
- 3) The west part of Qinba found a higher ratio value and a lower ratio found in the east part of the Qinba mountain.

## Abbreviations

MER	Mountain Equivalent Rainstorm.
TRMM	Tropical Rainfall Measuring Mission
NASA	National Aeronautics and Space Administration, USA
JAXA	Japan Aerospace Exploration Agency
VIRS	Visible Infrared Radiometer
TMI	TRMM Microwave Image
CERES	Cloud and Earth Radiant Energy Sensor
LIS	Lightning Imaging Sensor
PR	Precipitation Radar
TMPA	TRMM' Multi-Satellite Precipitation Analysis Products

## Acknowledgments

The authors thank Pro. Song Songbai for assistance with

partly theoretical work. The research was supported by the National Natural Science Foundation of China Project "Research on the Random Modeling and Prediction Method of the Non-stationary and Strong fluctuation sequence of Hydrology in a Changing Environment" (52079110).

## Author Contributions

**Khem Chunpanha:** Conceptualization, Data curation, Formal Analysis, Software, Writing – original draft

**Yan Baowen:** Funding acquisition, Methodology, Project administration, Resources, Supervision, Writing – review & editing

## Conflicts of Interest

The authors declare no conflicts of interest.

## References

- [1] He B-R, Zhai P-M. 2018. Changes in persistent and non-persistent extreme precipitation in China from 1961 to 2016. *Advances in Climate Change Research*, 9: 177-184. <https://doi.org/10.1016/j.accre.2018.08.002>
- [2] Gu X, Ye L, Xin Q, Zhang C, Zeng F, Nerantzaki SD, Papalexioiu SM. 2022. Extreme Precipitation in China: A Review on Statistical Methods and Applications. *Advances in Water Resources*: 104144. <https://doi.org/10.1016/j.advwatres.2022.104144>
- [3] NIC. 2009. China: The Impact of Climate Change to 2030 A Commissioned Research Report.
- [4] Duan W, Hanasaki N, Shiogama H, Chen Y, Zou S, Nover D, Zhou B, Wang Y. 2019. Evaluation and future projection of Chinese precipitation extremes using large ensemble high-resolution climate simulations. *Journal of Climate*. 32: 2169-2183. <https://doi.org/10.1175/JCLI-D-18-0465.s1>
- [5] Shao Y, Mu X, He Y, Sun W, Zhao G, Gao P. 2019. Spatial-temporal variations of extreme precipitation events at multi-time scales in the Qinling-Daba mountains region, China. *Quaternary International*, 525: 89-102. <https://doi.org/10.1016/j.quaint.2019.07.029>
- [6] Zhiyuan D, Yao H, Zhong ZH. 2024. Summer extreme precipitation patterns and synoptic-scale circulation precursors over the Tibetan Plateau. *Science China Earth Sciences*. 67(05): 1625-1638. <https://doi.org/10.1007/s11430-023-1321-6>
- [7] Formetta G, Feyen LJGEC. 2019. Empirical evidence of declining global vulnerability to climate-related hazards. *Global Environmental Change*, 57: 101920. <https://doi.org/10.1016/j.gloenvcha.2019.05.004>
- [8] Paprotny D, Sebastian A, Morales-Nápoles O, Jonkman SNJNc. 2018. Trends in flood losses in Europe over the past 150 years. *Nature Communications*, 9: 1-12. <https://doi.org/10.1038/s41467-018-04253-1>

- [9] Wang X, Ding Y, Zhao C, Wang J. 2018. Validation of TRMM 3B42V7 Rainfall Product under Complex Topographic and Climatic Conditions over Hexi Region in the Northwest Arid Region of China. *Water*, 10. <https://doi.org/10.3390/w10081006>
- [10] Cheng Z, Chen X, Zhang Y, Jin L. 2020. Spatio-temporal evolution characteristics of precipitation in the north and south of Qin-ba Mountain area in recent 43 years. *Arabian Journal of Geosciences*, 13. <https://doi.org/10.1007/s12517-020-05860-3>
- [11] Weidinger JT, Wang J, Ma N. 2002. The earthquake-triggered rock avalanche of Cuihua, Qin Ling Mountains, PR of China—the benefits of a lake-damming prehistoric natural disaster. *Quaternary International*, 93: 207-214. [https://doi.org/10.1016 /s1040-6182\(02\)00019-8](https://doi.org/10.1016 /s1040-6182(02)00019-8)
- [12] Qiu H, Cui Y, Pei Y, Yang D, Hu S, Wang X, Ma S. 2019. Temporal patterns of non-seismically triggered landslides in Shaanxi Province, China. *Catena*, 187. <https://doi.org/10.1016/j.catena. 2019.104356>
- [13] Khem, C., Yan, B. and Ouk, S. 2021. Applicability of TRMM Precipitation Product in Qinba Mountainous Area of Shaanxi Province. *Journal of Water Resource and Protection*, 13, 1076-1091. <https://doi.org/10.4236/jwarp.2021.1312058>
- [14] Huffman GJ, Bolvin DT, Nelkin EJ, Wolff DB, Adler RF, Gu G, Hong Y, Bowman KP, Stocker EF. 2007a. The TRMM multi-satellite precipitation analysis (TMPA): Quasi-global, multiyear, combined-sensor precipitation estimates at fine scales. *Journal of Hydro-meteorology*, 8: 38-55. <https://doi.org/10.1175/JHM560.1>
- [15] He Xiangfeng, Xue Qin. 2013. Mountain Equivalent Rainfall. *Meteorological Science and Technology*, 41(04): 771-776. <https://doi.org/10.19517/j.1671-6345.2013.04.029>
- [16] Jeonghoon L, Okjeong L, Jeonghyeon C, Jiyu S, Jeongeun W, Suhyung J, Sangdan Kim. 2023. Estimation of Real-Time Rainfall Fields Reflecting the Mountain Effect of Rainfall Explained by the WRF Rainfall Fields. *Water*, 15(9), 1794. <https://doi.org/10.3390/w15091794>
- [17] He S, Wang J, Liu S. 2020. Rainfall Event–Duration Thresholds for Landslide Occurrences in China. *Water*, 12. <https://doi.org/10.3390/w12020494>
- [18] Thoảng Trần Thanh, Tài La, Quân Trịnh Vĩnh, Long Nguyễn Bạch, Văn Sao Trần, Huy Trần Quốc, Trung Nguyễn Minh, Văn Ty Trần, Thành Nguyễn Trường, Kumar Pankaj, Văn Duy Đình, Downes Nigel K., Minh Huỳnh Vương Thu. 2022. Assessment of Potential Rainfall Distribution Patterns and Their Relationship with Inundation in Tra Vinh Province, Vietnam. *Journal of Climate Change*, 8(4). <https://doi.org/10.3233/JCC220030>